



HAL
open science

Novel approach for emergency dosimetry: Investigations of screen protectors for smartphones by EPR spectroscopy

M. Mobasher, N. Ollier, B. Gratuze, François Trompier

► To cite this version:

M. Mobasher, N. Ollier, B. Gratuze, François Trompier. Novel approach for emergency dosimetry: Investigations of screen protectors for smartphones by EPR spectroscopy. *Radiation Measurements*, 2024, 176 (6), pp.107218. 10.1016/j.radmeas.2024.107218 . irsn-04634989

HAL Id: irsn-04634989

<https://irsn.hal.science/irsn-04634989>

Submitted on 4 Jul 2024

HAL is a multi-disciplinary open access archive for the deposit and dissemination of scientific research documents, whether they are published or not. The documents may come from teaching and research institutions in France or abroad, or from public or private research centers.

L'archive ouverte pluridisciplinaire **HAL**, est destinée au dépôt et à la diffusion de documents scientifiques de niveau recherche, publiés ou non, émanant des établissements d'enseignement et de recherche français ou étrangers, des laboratoires publics ou privés.



Distributed under a Creative Commons Attribution - NonCommercial - NoDerivatives 4.0 International License



Novel approach for emergency dosimetry: Investigations of screen protectors for smartphones by EPR spectroscopy

M. Mobasher^{a,b}, N. Ollier^b, B. Gratuze^c, F. Trompier^{a,*}

^a *Institute for Radiological Protection and Nuclear Safety (IRSN), Fontenay-aux-roses, France*

^b *Laboratoire des Solides Irradiés Ecole Polytechnique, CNRS, CEA\DRF\IRAMIS, Institut Polytechnique de Paris, 91128, Palaiseau, France*

^c *Institut de Recherche sur Les Archéomatériaux Centre Ernest-Babelon CNRS/Univ, Orléans, France*

ABSTRACT

Screen protectors for smartphone are investigated in attempts for emergency dosimetry as for example in case of malicious attacks with radioactive sources or accidental overexposure. Electron Paramagnetic Resonance (EPR) measurements were carried out on six different types of screen protectors (SPs). The inter and intra batch variability of the EPR signals characteristics (sensitivity, stability, signal shape) were studied. Contrary to touch screen (De Angelis et al., 2015; Juniewicz et al., 2020), UVB exposure for SP is not a limiting confounding factor. All samples under irradiation exhibit same EPR signals. The nature of the radio-induced point defects was identified (HC₁ and HC₂) as well as their evolution according to dose. The linear dose response was studied in the 0–5 Gy dose range with a detection limit estimated of 750 mGy with a field deployable benchtop EPR spectrometer. Large variability of the dose response prevents presently from using universal calibration curve. Therefore, further work is needed to consider possible application for triage in the case of large-scale accidents scenarios.

1. Introduction

This work has been conducted to develop new capacity of dose estimation for individuals in case of radiological exposure, with a special motivation to fill the capacity gap for the so-called large-scale accident scenario for which no actual method of retrospective dosimetry fits the estimated needs. Nowadays, there is an emerging risk of malicious radiological attacks or accidental use of radioactive materials which led authorities to envision scenarios of large-scale radiological events with external exposure leading to acute radiation syndrome (Alexander et al., 2007; Coleman et al., 2015, 2019; Bailiff et al., 2016; ICRU, 2019). There is an international consensus that, in such a case, the current capacity of all retrospective dosimetry methods, mainly biological dosimetry, used to sort the exposed population with a view to medical treatment, would be largely exceeded (ICRU, 2019). It is therefore necessary to increase capacity, either with established and validated techniques, for example by developing networks of measurement laboratories, as for example with RENE network (Monteiro Gil et al., 2017), or, as in the specific case of cytogenetics, new automated image analysis methods based on artificial intelligence (ICRU, 2019). However, even by improving certain aspects of proven techniques, some of the bottlenecks inherent in these techniques will keep capacity well below what could be required (Monteiro Gil et al., 2017). It is therefore necessary to consider new approaches, in particular approaches that could also be deployable

in the field as close as possible to the victims, at the point of care. The use of electron paramagnetic resonance (EPR) spectroscopy is one of the techniques being considered to develop new capabilities. This technique has already been used to determine a person's level of exposure using biopsies of bone or tooth enamel, nail clippings or material from clothing or personal objects (glasses, glass watches, LCD glass, sugars, etc.) (Trompier et al., 2009; ICRU, 2019; Fattibene et al., 2023). For example, the Q-band EPR approach, which minimizes the sample size needed for analysis to 2–5 mg for enamel, minimizing the invasiveness of samples and still enables detection doses as low as 200–400 mGy with measurement times of approximately 5–10 min. This approach has been successfully used for two radiological accidents (in Bulgaria in 2011 and in Peru in 2012) (ICRU, 2019). Small mass biopsies of calcified tissue can also be measured with a higher sensitivity in Q-band (34 GHz) than in the conventional X-band (9.8 GHz) EPR (De et al., 2013; Romanyukha et al., 2014). As there is no need for sample preparation, samples can be measured as soon they are received. Considering that for triage mode, a single EPR measurement of 5 min would sufficient, one can estimate the daily initial capacity of about 100–150 samples per day and per spectrometer. Nevertheless, this capacity is not field deployable and only available in very few laboratories making this approach far to meet the capacity need for large scale event triage, even if overall larger than biological dosimetry. Both approaches require collecting and transporting biological samples in relatively large quantities, which requires

* Corresponding author.

E-mail address: francois.trompier@irsn.fr (F. Trompier).

a substantial and complex operational organization. The in vivo EPR measurement of teeth because it can be deployed in the field, can be considered complementary, even if the detectable dose levels still remain for the moment about 1 Gy in the best case, while considering the necessary presence of qualified personnel in number for the use of spectrometers (Swarts et al., 2018). Overall, even considering all the improvements and new methods, the overall capacity does not.

Nevertheless, one other alternative method based on EPR measurement of touchscreen of smartphone, was initially studied and evaluated within the EC funded Multibiodose project (Jaworska et al., 2014) and could possibly meet these requirements. As a matter of fact, alkali-aluminosilicate glass from touch screen of smartphone is one of the materials that could possibly be used also for large scale accident situations (Fattibene et al., 2014). Firstly, as almost all the population is equipped with a smartphone, one can consider that all individuals possibly involved in a large-scale accident would be supplied with a kind of fortuitous and ubiquitous dosimeter, its own smartphone. Secondly, smartphone touchscreen can be measured in situ by L-band EPR without removing a piece of screen or dismantling the phone (Trompier, 2016). Alternatively, small benchtop X-band spectrometers supplied with auto-sampler to measure small, scratched pieces of glass (100 mg) could already be foreseen to develop mobile laboratory units with sufficient sensitivity of measurement. The main drawbacks of this approach are that the glass used in smartphone touch screens are technological materials in permanent evolution and sampling operation even a small piece of glass may damage the smartphone and required also additional manpower and dedicated organization. A new brand of touch screen glass is released in average almost every one-two years. The approach has been evaluated with the first generations of tempered glass used in touch screen, namely Gorilla® Glass generation 1 and 2 and has been found suitable for dosimetry applications (Trompier et al., 2012; Fattibene et al., 2014; Juniewicz et al., 2020). Nevertheless, new generations with different composition present very different properties. That would require to study and characterize every new generation released, with the possibility that new generation does not response properly to dose. On the other hand, less technological progress is observed for other glasses such as those used for the screen protectors (SP) which is used to protect touchscreen of the smartphone against scratches and high-impact damage (added on top of the touchscreen). The composition of this glass, simpler from a technological point of view, can be expected to not evolve in time or depending on the suppliers. Moreover, the phone is not damaged when collecting the sample and sample collection is far easier and faster than for the touch screen. Even if not all phones are not supplied with SP, some sources indicate, that about 72 % of smartphone consumers use a screen protector in USA (“A Better Future for Screen Protection”). In this study, we investigated different types of screen protectors using EPR spectroscopy. One type of screen protector was considered as representative of this type of glass (labelled screen protector 3 (SP3)) after having observed the nature of point defects created for the six different types of screen protectors investigated through our batch studies. Different experiments were carried out including effect of dose, signal fading post-irradiation, reproducibility, variability and dose response.

2. Materials and methods

2.1. Sample origins

Six different types of SPs were investigated labelled as SP1, SP2, SP3, SP4, SP5 & SP6 from four different manufacturing companies. Their details are shown in Table 1. An image of the investigated samples is also shown in Supplementary Fig. 1. The screen protectors are described as tempered glass with an index of hardness of 9H except for SP4 (Tiger Glass) of 9H + hardness which is investigated thoroughly for our batch study.

Table 1
Details of the screen protectors investigated.

Screen protector labelling	Company, Glass type, phone model corresponding to the screen protector under investigation	Number of sheets investigated
SP1	Tempered Glass for Samsung A20e	1
SP2	Bigben, Tempered Glass for iPhone SE, iPhone5C/5S/5	1
SP3	Bigben, Tempered Glass for Samsung Galaxy A13 4G/A23 5G	1
SP4	Tiger Glass, Anti-bacterial Tempered Glass for iPhone 13 pro max	8
SP5	Bigben, Tempered Glass for Honor X7	1
SP6	Made for Xiaomi, Tempered Glass for Redmi 9C, Redmi 10 A	1

2.2. Sample preparation

Each SP is bent until breaking and the glass pieces were extracted by using forceps. Glass pieces were then cut into small pieces of about 1–5 mm in size to fit into the EPR measurement tubes. Samples were washed with ethanol to remove any traces of glue. The overall glass pieces from each SP were then mixed and split in aliquot of mass of 100–200 mg per sample for each respective type.

2.3. Sample irradiation

Irradiations of samples with high energy X-rays were performed free in air, under electronic equilibrium, using a medical linear accelerator (LINAC) supplied by Elekta with 10 MV X-rays. Reference dosimetry was performed in terms of air kerma with an ionization chamber (0.125 cm³ PTW Semiflex Chamber Type 31010). Investigated doses were ranging from 0 to 500 Gy.

UV irradiations were performed with an UV lamp (UVP lamp 3UV) generating UV rays of 302 nm (UVB) with energy flux of 11.14 mW cm⁻² at 7 cm from the lamp surface. The UV dosimetry was performed using a UV dosimeter (Radiometer RM12 from Grobel company) calibrated at the primary standard German laboratory (PTB).

2.4. Sample chemical analysis

SP3 glass was chemically analysed by using laser ablation inductively coupled mass spectrometry (LA-ICP-MS) in IRAMAT (CNRS/Univ. Orléans).

2.5. EPR measurements

For EPR measurements, a continuous wave X-band (~9.8 GHz) Bruker E500 type spectrometer supplied with a high Q resonator (Bruker SHQ) was used.

In addition, a X-band Bruker/Magnetech MS5000 benchtop was used for dose response measurements of SP3 samples of around 220 mg mass to evaluate the performance of a field deployable spectrometer. Eight measurements were done per each dose with normalization to the intensity of the internal marker placed in the resonator.

All data presented are normalized to sample mass. Baseline corrections and background subtractions were performed using Origin® software with the exact parameters mentioned for each figure.

For the EPR signals evolution with time section, each point corresponds to an average of 3–5 measurements.

For the variability study section, each spectrum shown per each screen protector type prior or post irradiation is in fact an average of 10 spectra.

3. Results

3.1. EPR spectra

3.1.1. Radiation dose effect on EPR signals

First, we investigated the effect of dose on the paramagnetic point defects shape of EPR spectra in a dose range between 0 Gy and 500 Gy for SP3. Spectra were measured after almost 4 months following irradiation. To clearly observe the dose effect, the spectrum of background irradiation (0 Gy) is subtracted from all doses as represented in Fig. 1 (A). In Fig. 1 (B), normalized spectra are presented to visualize clearly the effect of dose on the spectrum shape and to determine the nature of the point defects created. A similar spectrum is observed for low doses range (5, 10 and 20 Gy presented as solid lines) in comparison to the high dose range (50, 100 and 500 Gy presented as dashed lines) which display a single spectrum shape for each dose range. In the low dose range, the signal is quasi-isotropic with g values ($g = 2.0086$ and $g = 2.00361$). The g values and the shape let us think that the EPR signals correspond to the convolution of EPR signature of HC₁ and HC₂ point defects (Griscom, 1984; Zatsopin et al., 2012). HC₁ point defect is a hole connected to a non-bridging oxygen in the presence of an alkali cation and HC₂ point defect is a hole which is localized onto two non-bridging oxygen atoms stabilized by the alkali cation nearby (Griscom, 1984; Zatsopin et al., 2012). Their spectra are displayed in Fig. 1 (C) which are obtained from (Zatsopin et al., 2012). The nature of these point defects is supported by the presence of two alkali ions in the glass matrix Sodium (Na) and Potassium (K). The average content of 11.6 wt % of Sodium oxide (Na₂O) and 5.5 wt % of Potassium oxide (K₂O) were determined from the LA-ICP-MS chemical analysis performed (The composition of SP3 is displayed in the annex).

For the high dose range, a shape evolution is observed with the progressive decrease of the g component at 2.00633 and a shift

(indicated by the arrow in Fig. 1(B)) is noticed for the spectral shape between the low dose range (solid lines) and the high dose range (dashed lines). This evolution can be interpreted as a diminution of the HC₂/HC₁ ratio from 20 to 50 Gy and a progressive small increase from 50 to 500 Gy but this ratio remains lower than for the 5–20 Gy range (Zatsopin et al., 2012). However, a precise quantification of HC₁ and HC₂ would require a more precise fitting.

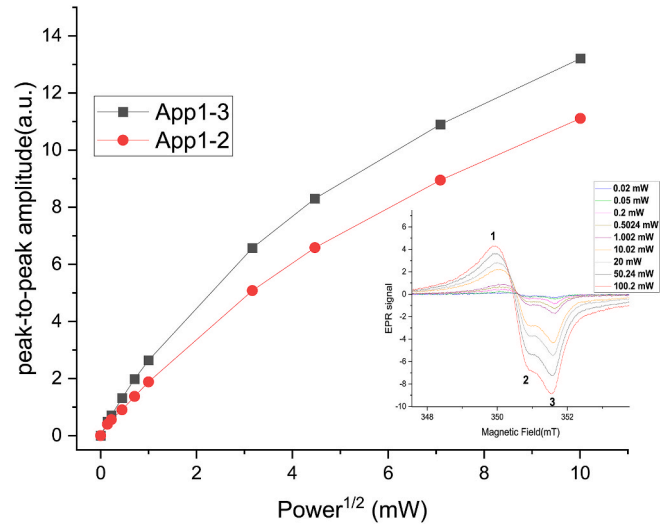


Fig. 2. Evolution of the peak-to-peak amplitude (1–2 & 1–3) with the square root of microwave power applied. Inset figure shows the spectra of 100 Gy irradiated SP3 sample with varying powers.

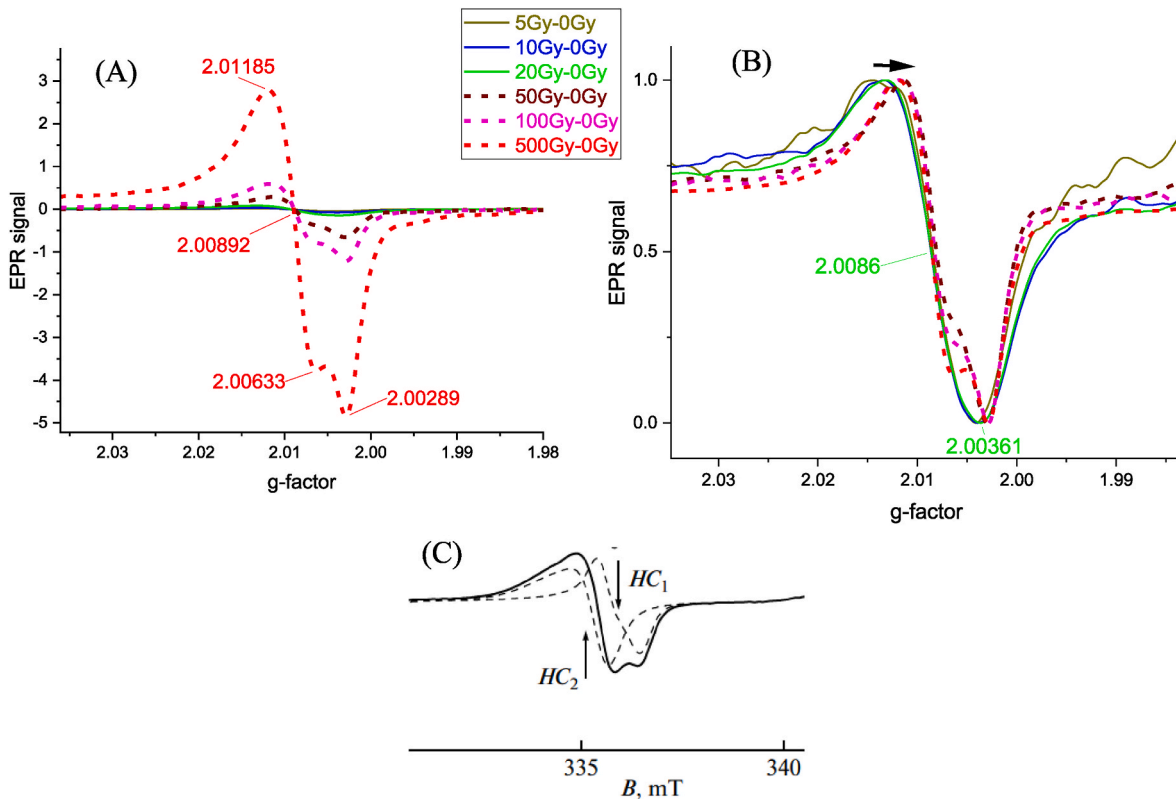


Fig. 1. (A) EPR spectra after subtraction of the background spectrum for low dose range (solid lines) and high dose range (dashed lines). (B) Normalization of maximal peak-to-peak amplitude (App) to 1 of the subtracted spectra for low dose range (solid lines) and high dose range (dashed lines). Spectra are obtained at 1 mW with 15 mT sweep width and 0.3 mT modulation amplitude. (C) HC₁ and HC₂ spectra which are presented in (Zatsopin et al., 2012).

3.1.2. Study of microwave power on EPR signals

Fig. 2 shows the variation of the peak-to-peak amplitude (App) of the 2 components identified for the 100 Gy irradiated SP3 sample as a function of the square root of the microwave power. The inset in Fig. 2 displays the spectra obtained at the different powers investigated following stabilization with the points taken for the App values (1–2 & 1–3).

After fitting the App evolution for these 2 curves according to the following equation:

$$I = \frac{a\sqrt{P}}{\left(1 + \frac{P}{P_{sat}}\right)^b} \quad (\text{Eq. 1})$$

The micro-wave saturation power and the extracted parameters are presented in Table 2.

The App (1–2) signal is linked to HC₂ while App (1–3) signal is linked to HC₁. The respective saturation powers are determined to be 5.49 and 3.31 mW. Those values are in agreement with the micro-wave powers used for measurements in (Griscom, 1984) and (Zatsepin et al., 2012) which are less than 1 mW and 2 mW respectively.

According to (Griscom, 1984), HC₁ point defect saturates at lower power compared to HC₂ and that agrees with our results.

3.1.3. EPR signals evolution with time

An important aspect for dosimetry concerns the EPR signal stability of the samples which basically decreases with time due to point defect fading. As shown in Fig. 3 (A), the evolution of the App maxima (1–3 as stated in the inset of Fig. 2) of 100 Gy irradiated sample is plotted against time (in days) after the irradiation. A second order exponential decay function was used to fit the evolution of App with time. This indicates the presence of at least two-point defects originating the signal obtained at 100 Gy supporting our hypothesis of the presence of two main defects (HC₁ and HC₂). In Fig. 3(B), averaged spectra of 100 Gy SP3 sample are plotted for measurements done on the day of irradiation (dashed line) and a month post irradiation (solid line) in order to show its evolution with respect to time. Following these results, we estimated that 8 days duration post irradiation is needed for the EPR spectra stabilization. Indeed, the signal decreases by almost 35% during this period which agrees with Pukhkaya et al. (2013) showing a 40% loss of the signal during the 1st week post irradiation in Na-alumino-silicate glasses.

3.2. Variability study

3.2.1. Inter batch variability study

Initially, we observed the similarity between the EPR spectra obtained for 5 out of the 6 types of screen protectors (SP2, SP3, SP4, SP5 and SP6) investigated prior to any irradiation (0 Gy) which are shown in Supplementary Fig. 2. To minimize the effect of the background signal, we irradiated the 6 screen protectors at a high dose of 200 Gy for the sake of comparison between them. The EPR spectra are shown in Fig. 4 (A). The shape of all SPs is quite similar to SP3 high dose range presented in Fig. 1(A) except SP2. We can therefore deduce that HC₁ and HC₂ point defects (Griscom, 1984; Zatsepin et al., 2012) are created in all 6 types. However, the shape of SP2 infers a lower HC₂/HC₁ ratio than the others, may be due to different alkali ions content. After obtaining a mean value for the amplitude peak to peak of the maxima for all these spectra, we

Table 2

Fitting parameters for the App of SP3 irradiated at 100 Gy with respect to power evolution.

SP3 dose/App	Micro-Wave Saturation Power P _{sat} (mW)	a	b
100 Gy/App (1–3)	3.31	2.86	0.23
100 Gy/App (1–2)	5.49	1.98	0.20

plotted the relative difference to this mean to visualize the difference in percentage as seen in Fig. 4 (B) for the 6 types. The resulting relative standard deviation (RSD) was determined to be 34% indicating a large variation between the amplitude peak to peak values of the 6 types of SPs. Nevertheless, we chose SP3 to be a representative for our detailed analysis since the same nature of point defects is observed for all of them and its difference to the mean of the 6 types is one of the lowest (13%).

3.2.2. Intra batch variability study (0 Gy & 100 Gy)

Additionally, we studied the variability between different samples coming from the same batch of screen protector, both for background and post irradiation signals. In addition, we collected samples from the edges and the center part of each sample to compare the effect of location of the sample on the resulting background signal obtained. We tested 8 samples of screen protector 4 (SP4) as seen in Supplementary Fig. 3. They are referred to as SP4_1, SP4_2, SP4_3 ... and SP4_8 respectively. The EPR spectra of the center and the edges of each 0 Gy sample are displayed in Fig. 5 (A, B) respectively and of the 100 Gy samples in Fig. 5 (C). Based on these results, we can deduce that there is no effect on the spectral shape and intensity independent of the sample location in the glass sheet. This is further confirmed after calculating the relative difference (%) from the mean App value per each group (center 0 Gy, edge 0 Gy and 100 Gy samples) as a percentage which is shown in Fig. 6. The relative standard deviation (RSD) is calculated for the 3 groups and there is a decrease in the post irradiation value due to the presence of a more intense signal.

3.3. Dose response

3.3.1. X-ray dose response (0–5 Gy)

The investigated doses are: 0, 1, 2, 3 and 5 Gy with the SP3 representative sample measured with a field deployable benchtop spectrometer. The dose response curve is shown in Fig. 7, it was obtained following stabilization of the radio-induced signals. The dose response is found to be linear in the dose range investigated. The detection limit (DL) and the critical dose (CD) were respectively found to be 755 and 392 mGy with the method of calculation used in (Fattibene et al., 2014).

3.3.2. UV effect and duration response

One of the confounding factors investigated for glass samples previously studied (De Angelis et al., 2015; Juniewicz et al., 2020) is UV effect. As a matter of fact, sometimes the UV induced signal overlaps with the radio-induced signal altering the dose estimation. Fig. 8 shows the difference between the UV irradiated SP3 sample for 3 h (solid line) in comparison to that of the background (0 Gy presented as dashed line). As a result, we observed that the signal generated by UV peaking at $g = 1.9743$ and $g = 1.9317$ is different from the radio-induced signal (around $g = 2$) (as observed in Fig. 1). The UV induced signal does not correspond to a point defect and could correspond to Zr³⁺ ions ($g = 1.93$) evidencing a possible reduction of Zr⁴⁺ ions under UV (Gac et al., 2017; Griscom and Ginther, 1989). This interpretation is supported by the chemical analysis showing the presence of Zr in SP3 glass (Zirconium oxide (ZrO₂) content is 0.694 wt %).

In Fig. 9, the amplitude of the UV signal of these averaged measurements (8 measurements) is shown as a function of the specified duration (0.5, 1, 2, 3 and 4 h). Starting from 2 h of irradiation a saturation of the UV signal is observed. An allometric growth function is used to fit the App of UV signal as a function of duration of UV exposure.

4. Discussions

A lot of research is carried out on different materials in attempts to determine the dose received by the victims in case of radiological accidents. Those can be biological materials or materials (Marciniak et al., 2022) carried by the victim like plastics (Trompier et al., 2010), touch screens (Trompier et al., 2011; Sholom and McKeever, 2017; Juniewicz

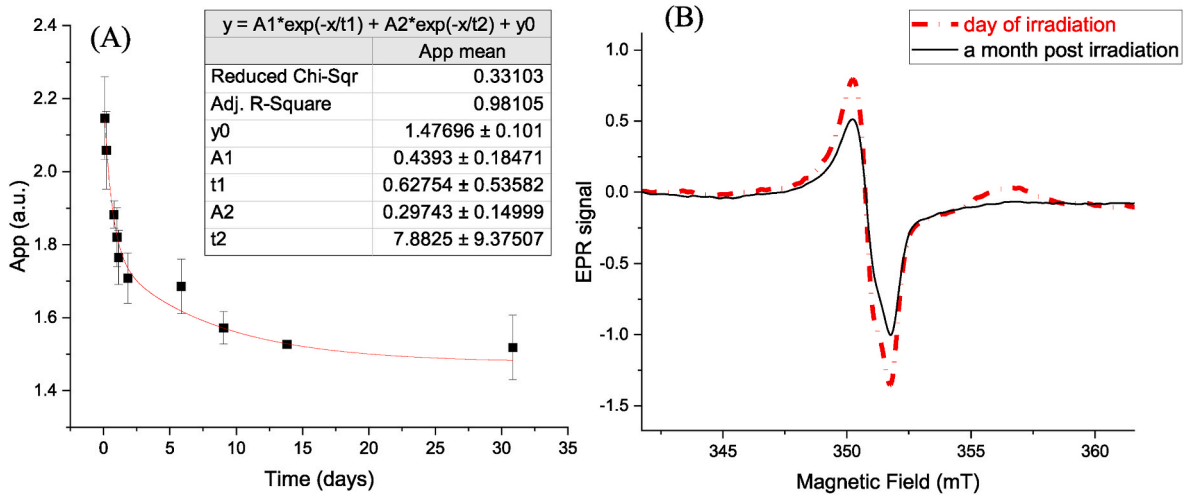


Fig. 3. (A) Evolution of average of App with time for SP3 100 Gy sample fitted with a 2nd order exponential decay function. (B) Averaged spectra obtained on the day of irradiation (dashed line) in comparison to 1 month post irradiation (solid line) Spectra are measured at 1 mW with 0.3 mT modulation amplitude.

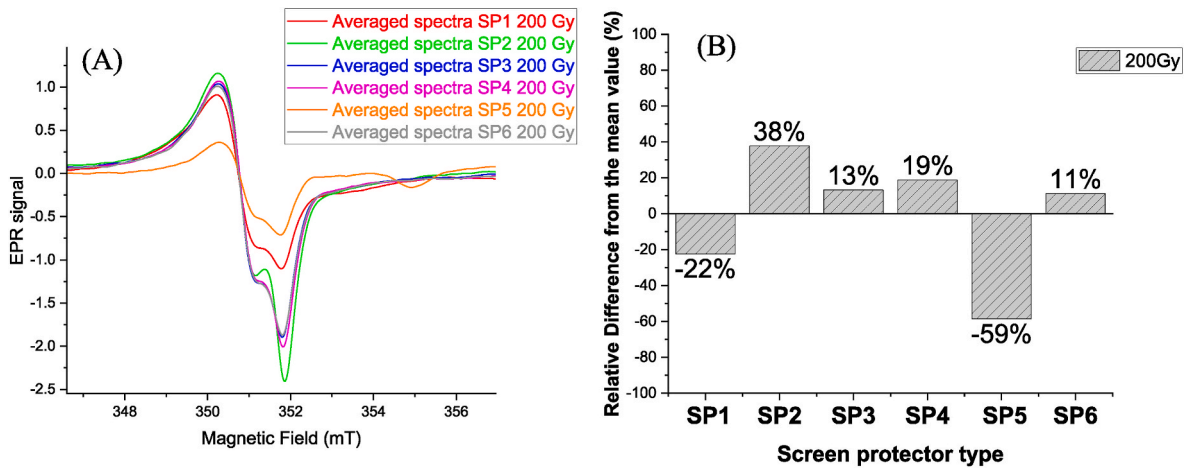


Fig. 4. (A) Averaged EPR spectra of 6 different types of screen protectors post stabilization of 200 Gy X-ray irradiation. (B) Relative difference (%) from mean value of App for the 6 types. Spectra are measured at 1 mW with 0.3 mT modulation amplitude.

et al., 2019) laboratory or window glass (Teixeira et al., 2005; Gancheva et al., 2006), or lens of eyeglasses (Tuner, 2023). In this study, we presented according to our knowledge, the first EPR results on dosimetry characterization of screen protectors. We show good results for the dose response curve for one sample (SP3) obtained by X-band EPR benchtop with a DL estimated at 750 mGy which could be used on site of the accident improving the dose limit compared to what has been previously reported for different types of glass with 2 Gy DL (Trompier et al., 2009; Sholom and McKeever, 2017; Sholom et al., 2019).

Our results are in line with the DL and CD calculated from calibration curves of participants to an intercomparison on Gorilla® Glass generation 2 (Fattibene et al., 2014). In this work, for homogenised glass samples, DL and CD were respectively ranging between 740 and 790 mGy, and 370 and 400 mGy. It is worth noting that these results were obtained with large EPR X-band spectrometer only available at the laboratory. For heterogeneous samples, DL were found to be ranging from 2.9 Gy up to 11 Gy (Fattibene et al., 2014). This latter finding underlines the importance of dose response variability among samples of glass even from the same type and its impact on DL. Although, we observe the same nature of point defects created for the six irradiated SP samples at 200 Gy, the large variability between the resulting App makes it difficult to build a universal calibration curve for dose estimation. Nevertheless, very small variation is noted for the batch study

done on SP4 whether for its background signal or post irradiation which shows the robust possibility of using screen protectors as dosimetric estimation for small scale accidents if the type of SP is known. A calibration curve established with samples from different SP will probably be associated with larger DL and CD than we report here. Our DL and CD estimation must be considered as a best-case performance for a benchtop spectrometer. Nevertheless, it demonstrates that field deployable benchtop spectrometer is a promising approach that needs to be considered. In addition to the field deployability approach, it is worth noting that auto-sampler can be inserted on that type of device that would minimize the manpower needed to manage EPR measurements.

In support of previous studies done on the fading of radio-induced signal from glass of mobile phones by more than 30% during the first 6–8 days post irradiation (Bassinot et al., 2010; Trompier et al., 2011; Juniewicz et al., 2019; McKeever et al., 2019; Marciniak et al., 2022), the same duration is observed for SP3 with 35% decay of the original signal after 8 days. This duration gives us the time delay in which the measurement for dose estimation has to be performed to minimize variation when dose response curves are established or when samples with unknown dose and without information on time of irradiation have to be analysed. If results have to be provided in short delay, a procedure of heating the sample could be set-up to obtain quickly a signal stabilization. Also, if the time of irradiation is not known, multiple

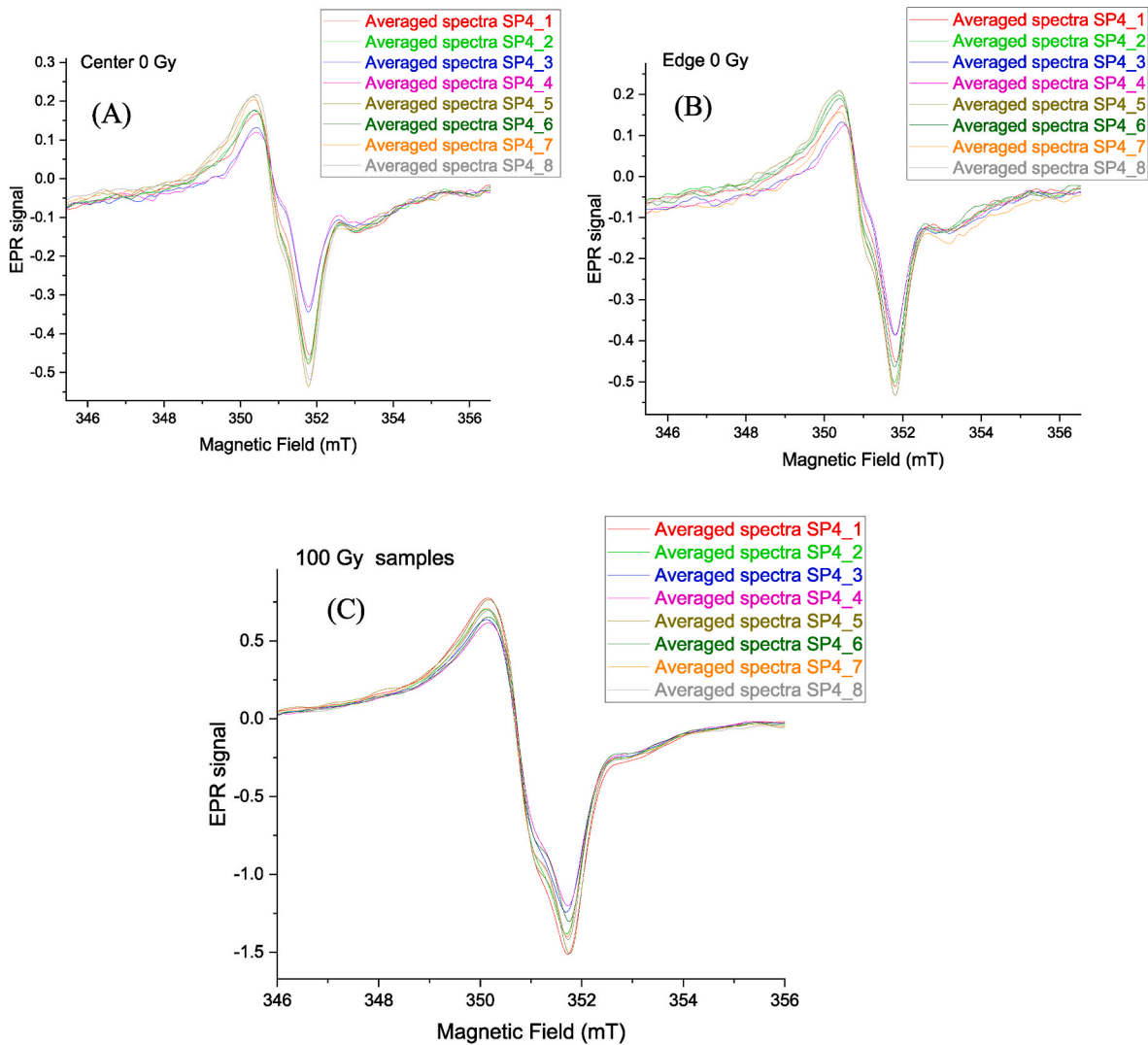


Fig. 5. Averaged EPR spectra of center (A) and edge (B) samples for the batch study of SP4 prior to any irradiation (0 Gy) (8 samples). (C) Averaged EPR spectra for 100 Gy SP4 irradiated samples. Spectra are obtained at 1 mW with 0.3 mT modulation amplitude.

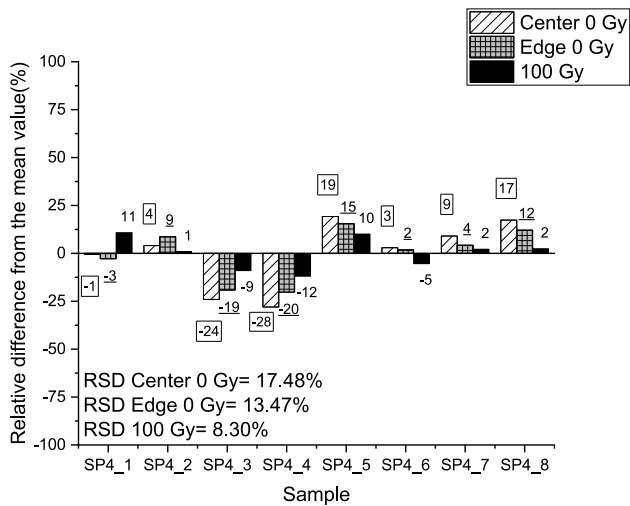


Fig. 6. Relative difference (%) from mean value of App for each group (center 0 Gy, edge 0 Gy & 100 Gy). Relative standard deviation (RSD) is displayed for each group.

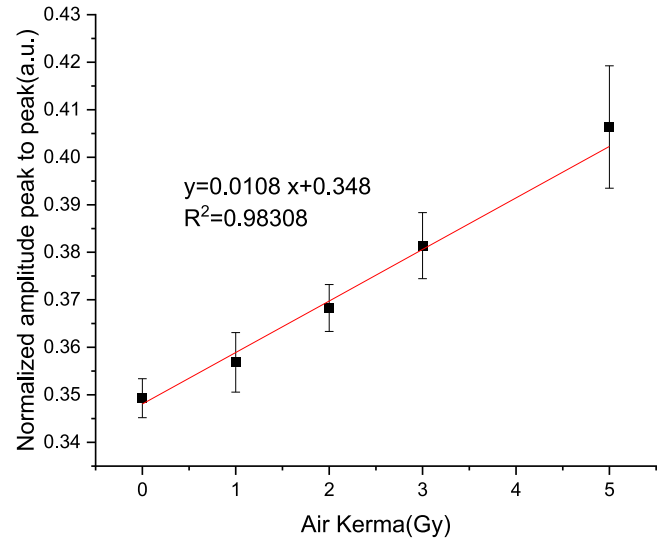


Fig. 7. Linear dose response for SP3 between 0 and 5 Gy. Spectra are obtained at 1.995 mW with 0.7 mT modulation amplitude.

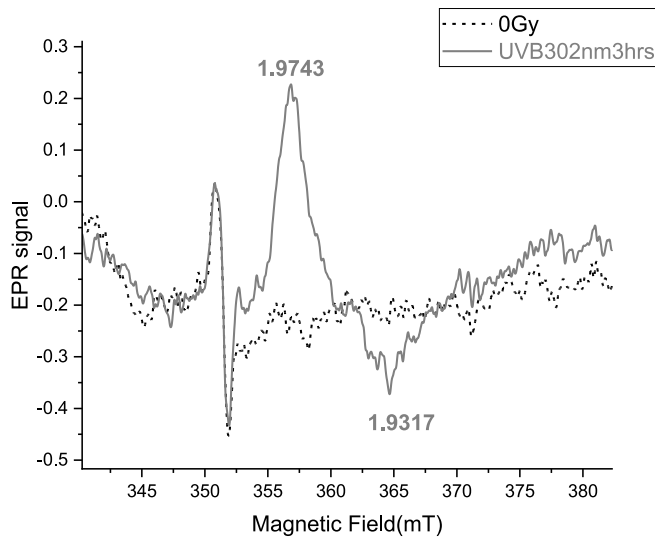


Fig. 8. EPR spectra of 0 Gy (dashed line) and UVB302nm 3hrs (solid line) samples with g-factors indicated for the UVB irradiated sample. Spectra are obtained at 2 mW with 0.3 mT modulation amplitude.

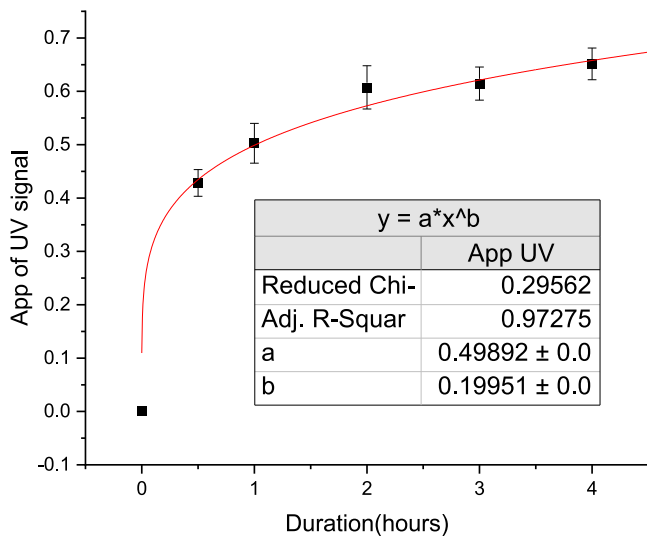


Fig. 9. The averaged App of UV irradiation is plotted against the exposure duration. Spectra are obtained at 2 mW with 0.3 mT modulation amplitude.

measurement at different times could possibly provide an indication on

Annex

Table 1
Chemical composition results by LA-ICP-MS for SP3.

Oxide	weight (%)
Silicon dioxide (SiO ₂)	61.30
Aluminium oxide (Al ₂ O ₃)	14.43
Sodium oxide (Na ₂ O)	11.67
Potassium oxide (K ₂ O)	5.51
Zirconium (IV) oxide (ZrO ₂)	0.694
Magnesium oxide (MgO)	6.15

irradiation time. This information in the context -for example, of an insidious exposure scenario-could be of interest for the medical team in charge of individuals who had been severely exposed.

In addition, contrarily to Gorilla® glass 2 for example (De Angelis et al., 2015), there is no overlap between the signal induced by UV and the radio-induced signal by X-ray irradiation unlike many other publications regarding glass where UV had an influence on the radio-induced signal (De Angelis et al., 2015; Juniewicz et al., 2020).

4.1. Conclusions and future perspectives

In this study, we performed different experiments to study the possibility of usage of screen protector glasses (SP) for dosimetric investigations. Among the results, we attribute the EPR signal to HC₁ and HC₂ point defects and the ratio of HC₂/HC₁ depends on the dose. The batch investigations between 6 different types of SPs showed the variability between them. On the other hand, we concluded that -for one type of SP- there is no effect on the location of samples' collection prior or post irradiation. UV induced a new signal attributed to Zr³⁺ ions that does not overlap with the radio-induced signal around g = 2. Considering the variability on dose response, we concluded that a universal calibration is not a suitable approach and further work is needed to consider possible application for large-scale accidents and triage. However, SP3 showed a linear dose response curve for the range of less than 5 Gy which could be likely used for small scale accidents with a DL estimated around 750 mGy.

CRediT authorship contribution statement

M. Mobasher: Writing – original draft, Methodology, Investigation, Formal analysis, Data curation. N. Ollier: Writing – review & editing, Validation, Supervision, Project administration, Conceptualization. B. Gratuze: Resources. F. Trompier: Writing – review & editing, Validation, Supervision, Project administration, Funding acquisition, Conceptualization.

Declaration of competing interest

The authors declare that they have no known competing financial interests or personal relationships that could have appeared to influence the work reported in this paper.

Data availability

Data will be made available on request.

Appendix A. Supplementary data

Supplementary data to this article can be found online at <https://doi.org/10.1016/j.radmeas.2024.107218>.

References

- A Better Future for Screen Protection [WWW Document], n.d. URL <https://www.gonimble.com/blogs/news/a-better-future-for-screen-protection>.
- Alexander, G.A., Swartz, H.M., Amundson, S.A., Blakely, W.F., Buddemeier, B., Gallez, B., Dainiak, N., Goans, R.E., Hayes, R.B., Lowry, P.C., Noska, M.A., Okunieff, P., Salner, A.L., Schauer, D.A., Trompier, F., Turteltaub, K.W., Voisin, P., Wiley, A.L., Wilkins, R., 2007. BiodosEPR-2006 Meeting: acute dosimetry consensus committee recommendations on biodosimetry applications in events involving uses of radiation by terrorists and radiation accidents. *Radiat. Meas.* 42, 972–996. <https://doi.org/10.1016/j.radmeas.2007.05.035>.
- Bailiff, I.K., Sholom, S., McKeever, S.W.S., 2016. Retrospective and emergency dosimetry in response to radiological incidents and nuclear mass-casualty events: a review. *Radiat. Meas.* 94, 83–139. <https://doi.org/10.1016/j.radmeas.2016.09.004>.
- Bassinnet, C., Trompier, F., Clairand, I., 2010. Radiation accident dosimetry on glass by tl and epr spectrometry. *Health Phys.* 98, 400–405. <https://doi.org/10.1097/01.HP.0000346330.72296.51>.
- Coleman, C.N., Sullivan, J.M., Bader, J.L., Murrain-Hill, P., Koerner, J.F., Garrett, A.L., Weinstock, D.M., Case, C., Hrdina, C., Adams, S.A., Whitcomb, R.C., Graeden, E., Shankman, R., Lant, T., Maidment, B.W., Hatchett, R.C., 2015. Public health and medical preparedness for a nuclear detonation: the nuclear incident medical enterprise. *Health Phys.* 108, 149–160. <https://doi.org/10.1097/HP.0000000000000249>.
- De Angelis, C., Fattibene, P., Quattrini, M.C., Della Monaca, S., Trompier, F., Wieser, A., Brai, M., Ciesielski, B., De Angelis, C., Della Monaca, S., et al., 2015. Variability of the dosimetric EPR response of Gorilla Glass touchscreen to dose and to light. Presented at the 2015 EPR BioDose Conference. Hanover, USA, October 4–8, 2015; Poster P8-W.
- De, T., Romanyukha, A., Trompier, F., Pass, B., Misra, P., 2013. Feasibility of Q-band EPR dosimetry in biopsy samples of dental enamel, dentine and bone. *Appl. Magn. Reson.* 44, 375–387. <https://doi.org/10.1007/s00723-012-0379-9>.
- Fattibene, P., Trompier, F., Bassinet, C., Ciesielski, B., Discher, M., Eakins, J., Gonzales, C.A.B., Huet, C., Romanyukha, A., Woda, C., Juniewicz, M., Kim, H., Lee, J., Marciniak, A., Sholom, S., Yasuda, H., 2023. Reflections on the future developments of research in retrospective physical dosimetry. *Phys. Open* 14. <https://doi.org/10.1016/j.physo.2022.100132>.
- Fattibene, P., Trompier, F., Wieser, A., Brai, M., Ciesielski, B., De Angelis, C., Della Monaca, S., Garcia, T., Gustafsson, H., Hole, E.O., Juniewicz, M., Krefft, K., Longo, A., Leveque, P., Lund, E., Marrale, M., Michalec, B., Mierzwińska, G., Rao, J. L., Romanyukha, A.A., Tuner, H., 2014. EPR dosimetry intercomparison using smart phone touch screen glass. *Radiat. Environ. Biophys.* 53. <https://doi.org/10.1007/s00411-014-0533-x>.
- Gac, A. Le, Boizot, B., Jégou, C., Peugot, S., 2017. Aluminosilicate glasses structure under electron irradiation: an EPR study. *Nucl. Instrum. Methods Phys. Res. Sect. B Beam Interact. Mater. Atoms* 407, 203–209. <https://doi.org/10.1016/j.nimb.2017.06.025>.
- Gancheva, V., Yordanov, N.D., Karakirova, Y., 2006. EPR investigation of the gamma radiation response of different types of glasses. *Spectrochim. Acta Part A Mol. Biomol. Spectrosc.* 63, 875–878.
- Griscom, D.L., 1984. Electron SPIN resonance studies of trapped hole centers in irradiated alkali silicate glasses: a critical comment on current models for HC I and HC 2. *J. Non-Cryst. Solids* 64, 229–247.
- Griscom, D.L., Ginther, R.J., 1989. Electron spin resonance determination of the redox state of iron and its relationship to radiation-induced defect centers in oxidized and reduced ZrF4-based glasses. *J. Non-Cryst. Solids* 113, 146–160. [https://doi.org/10.1016/0022-3093\(89\)90005-7](https://doi.org/10.1016/0022-3093(89)90005-7).
- ICRU, 2019. Methods for initial-phase assessment of individual doses following acute exposure to ionizing radiation. *J. ICRU Rep.* 94 19 (1), 1–162.
- Jaworska, A., Ainsbury, E.A., Fattibene, P., Lindholm, C., Oestreicher, U., Rothkamm, K., Romm, H., Thierens, H., Trompier, F., Voisin, P., Vral, A., Woda, C., Wojcik, A., 2014. Operational guidance for radiation emergency response organisations in Europe for using biodosimetric tools developed in eu multibiodose project. *Radiat. Protect. Dosim.* 164, 165–169. <https://doi.org/10.1093/rpd/ncu294>.
- Juniewicz, M., Ciesielski, B., Marciniak, A., Prawdzik-Dampc, A., 2019. Time evolution of radiation-induced EPR signals in different types of mobile phone screen glasses. *Radiat. Environ. Biophys.* 58, 493–500. <https://doi.org/10.1007/s00411-019-00805-1>.
- Juniewicz, M., Marciniak, A., Ciesielski, B., Prawdzik-Dampc, A., Sawczak, M., Boguś, P., 2020. The effect of sunlight and UV lamp exposure on EPR signals in X-ray irradiated touch screens of mobile phones. *Radiat. Environ. Biophys.* 59, 539–552. <https://doi.org/10.1007/s00411-020-00858-7>.
- Marciniak, A., Ciesielski, B., Juniewicz, M., 2022. EPR dosimetry in glass: a review. *Radiat. Environ. Biophys.* 61, 179–203. <https://doi.org/10.1007/s00411-022-00970-w>.
- McKeever, S.W.S., Sholom, S., Chandler, J.R., 2019. A comparative study of epr and TL signals in Gorilla® glass. *Radiat. Protect. Dosim.* 186, 65–69. <https://doi.org/10.1093/rpd/ncy243>.
- Monteiro Gil, O., Vaz, P., Romm, H., De Angelis, C., Antunes, A.C., Barquinero, J.F., Beinke, C., Bortolin, E., Burbidge, C.I., Cucu, A., Della Monaca, S., Domene, M.M., Fattibene, P., Gregoire, E., Hadjidekova, V., Kulka, U., Lindholm, C., Meschini, R., M'Kacher, R., Moquet, J., Oestreicher, U., Palitti, F., Pantelias, G., Montoro Pastor, A., Popescu, I.A., Quattrini, M.C., Ricoul, M., Rothkamm, K., Sabatier, L., Sebastião, N., Sommer, S., Terzoudi, G., Testa, A., Trompier, F., Vral, A., 2017. Capabilities of the RENEB network for research and large scale radiological and nuclear emergency situations. *Int. J. Radiat. Biol.* 93, 136–141. <https://doi.org/10.1080/09553002.2016.1227107>.
- Norman Coleman, C., Bader, J.L., Koerner, J.F., Hrdina, C., Cliffer, K.D., Hick, J.L., James, J.J., Mansoura, M.K., Livinski, A.A., Nystrom, S.V., Dicarolo-Cohen, A., Marinissen, M.J., Wathen, L., Appler, J.M., Buddemeier, B., Casagrande, R., Estes, D., Byrne, P., Kennedy, E.M., Jakubowski, A.A., Case, C., Weinstock, D.M., Dainiak, N., Hanfling, D., Garrett, A.L., Grant, N.N., Dodgen, D., Redlener, I., MacKay, T.F., Treber, M., Homer, M.J., Taylor, T.P., Miller, A., Korch, G., Hatchett, R., 2019. Chemical, Biological, Radiological, Nuclear, and Explosive (CBRNE) Science and the CBRNE Science Medical Operations Science Support Expert (CMOSSE). *Disaster Med. 13. Public Health Prep*, pp. 995–1010. <https://doi.org/10.1017/dmp.2018.163>.
- Pukhkaya, V., Charpentier, T., Ollier, N., 2013. Study of formation and sequential relaxation of paramagnetic point defects in electron-irradiated Na-aluminosilicate glasses : in fl uence of Yb. *J. Non-Cryst. Solids* 364, 1–8. <https://doi.org/10.1016/j.jnoncrysol.2013.01.021>.
- Romanyukha, A., Trompier, F., Reyes, R.A., 2014. Q-band electron paramagnetic resonance dosimetry in tooth enamel: biopsy procedure and determination of dose detection limit. *Radiat. Environ. Biophys.* 53, 305–310. <https://doi.org/10.1007/s00411-013-0511-8>.
- Sholom, S., McKeever, S.W.S., 2017. Developments for emergency dosimetry using components of mobile phones. *Radiat. Meas.* 106, 416–422. <https://doi.org/10.1016/j.radmeas.2017.06.005>.
- Sholom, S., Wieser, A., McKeever, S.W.S., 2019. A comparison of different spectra deconvolution methods used in epr dosimetry with Gorilla® glasses. *Radiat. Protect. Dosim.* 186, 54–59. <https://doi.org/10.1093/rpd/ncy260>.
- Swarts, S.G., Sidabras, J.W., Grinberg, O., Tipikin, D.S., Kmieć, M.M., Petryakov, S.V., Schreiber, W., Wood, V.A., Williams, B.B., Flood, A.B., Swartz, H.M., 2018. Developments in biodosimetry methods for triage with a focus on X-band electron paramagnetic resonance in vivo fingernail dosimetry. *Health Phys.* 115, 140–150. <https://doi.org/10.1097/HP.0000000000000874>.
- Teixeira, M.I., Ferraz, G.M., Caldas, L.V.E., 2005. EPR dosimetry using commercial glasses for high gamma doses. *Appl. Radiat. Isot.* 62, 365–370. <https://doi.org/10.1016/j.apradiso.2004.08.012>.
- Trompier, F., Fattibene, P., Woda, C., Bassinet, C., Bortolin, E., De Angelis, C., Della Monaca, S., Viscomi, D., Wieser, A., 2012. Retrospective dose assessment in a radiation mass casualty by EPR and OSL in mobile phones. *Glasgow, UK, P- 02.30. In: The Proceedings of the 13th IRPA International Congress, 13–18 May 2012.*
- Trompier, F., Della Monaca, S., Fattibene, P., Clairand, I., 2011. EPR dosimetry of glass substrate of mobile phone LCDs. *Radiat. Meas.* 46, 827–831.
- Trompier, F., 2016. Procédé de dosimétrie de rayonnements ionisants par mesure RPE directe sur le verre d'un écran d'un appareil électronique. *WO 2016/055315 A1.*
- Trompier, F., Bassinet, C., Clairand, I., 2010. Radiation accident dosimetry on plastics by epr spectrometry. *Health Phys.* 98, 388–394. <https://doi.org/10.1097/01.HP.0000346334.78268.31>.
- Trompier, F., Bassinet, C., Wieser, A., Angelis, C. De, Viscomi, D., Fattibene, P., 2009. Radiation-induced signals analysed by EPR spectrometry applied to fortuitous dosimetry. *Ann. Ist. Super Sanita* 45, 287–296.
- Tuner, H., 2023. EPR dosimetric properties of different mineral eyeglass lenses. *Radiat. Phys. Chem.* 206, 110764. <https://doi.org/10.1016/j.radphyschem.2023.110764>.
- Zatsepin, A.F., Guseva, V.B., Vazhenin, V.A., Artoymov, M.Y., 2012. Paramagnetic defects in gamma-irradiated Na/K-silicate glasses. *Phys. Solid State* 54, 1776–1784. <https://doi.org/10.1134/S1063783412090326>.